

Phase transformations in porous Al_2O_3 ceramic nanoclusters

S Ram and S Rana*

Materials Science Centre, Indian Institute of Technology,
Kharagpur-721 302, West Bengal, India

E-mail : srana@matssc.iitkgp.ernet.in

Abstract : A porous ceramic powder of Al_2O_3 nanoclusters is deduced by a controlled thermal decomposition of a porous $\text{AlO}(\text{OH})\cdot x\text{H}_2\text{O}$ powder (porosity $\Phi = 18\%$), a precursor of alumina or sapphire, at selected temperatures in the 500-1500 K range. The precursor has been synthesized in a highly pure form using a new chemical method of an electrochemical surface hydrolysis of a thin Al-plate in water. The pores govern a controlled thermal decomposition of it at a molecular scale and result in a refined porous Al_2O_3 powder of an enhanced Φ value up to 40% over the starting value. The sample appears in different polymorphic metastable forms at different temperatures in this range. If compared to in a bulk Al_2O_3 , the present transformations occur at significantly reduced temperatures by the assistance of the pores. The results are discussed with microstructure and X-ray powder diffraction studies.

Keywords : Al_2O_3 , ceramic nanocluster, electrochemical surface hydrolysis, phase transformation

PACS Nos. : 82.80.Fk, 64.70.Nd

1. Introduction

Alumina (Al_2O_3) or sapphire forms an important series of ceramic materials with exceptional properties [1-5] such as great hardness, chemical inertness, and a high melting temperature. It has many industrial applications such as in catalysts, coatings, microelectronics, composite materials, and advanced material technology. Besides, the stable phase α - Al_2O_3 , it exists in a number of metastable polymorphs, e.g., γ - Al_2O_3 , δ - Al_2O_3 , θ - Al_2O_3 and ϵ - Al_2O_3 [6,7]. The structures of the metastable aluminas, also called transition aluminas, can be divided into two main categories based on either a fcc or a hcp arrangement of the atoms. Among them, γ - Al_2O_3 or θ - Al_2O_3 has a fcc structure while ϵ - Al_2O_3 or α - Al_2O_3 belongs to the hcp structure. In contrast to α - Al_2O_3 , there has been much less study on other phases, although they have their own importance in catalysts and other applications.

The recent development in synthesizing of porous Al_2O_3 ceramics and the porous Al_2O_3 reinforced composite materials have generated further new interest in this series [8,9]. They form a host for a uniform intercalation and dispersion of separated particles of pure metals or metal oxides of quantum confined size in the pores and form a variety of optical, magnetic and electronic devices [8-11]. Apart from the electronic applications, they are widely used in adsorption and catalysts where their

large surface area, pore structure and surface chemistry play an essential role [9-13]. A porous Al_2O_3 powder is a very useful precursor for synthesis of a porous cermet or other porous ceramic composites.

Several methods using sol-gel and other wet chemical methods are known for synthesis of pure Al_2O_3 ceramics [12-14]. A limitation of all these methods is that they do not give a porous Al_2O_3 powder with a desired porosity. Here, we report synthesis, thermal stabilities, and phase transformations in porous Al_2O_3 clusters. A new chemical method involving an electrochemical surface hydrolysis of a thin Al plate in a pure water [12, 13] and thermal annealing of the obtained product at elevated temperatures are used to synthesize the porous Al_2O_3 powders.

2. Experimental details

The Al_2O_3 nanoclusters in different polymorphic forms are obtained by a thermal decomposition of a porous $\text{AlO}(\text{OH})\cdot x\text{H}_2\text{O}$ precursor powder at selected temperatures, in the 500 to 1500K range, in air. The $\text{AlO}(\text{OH})\cdot x\text{H}_2\text{O}$ precursor had a porosity $\sim 18\%$ and was a pure better than 99.9%. It was obtained by an electrochemical surface hydrolysis of a pure (99.9%) Al-metal plate in a pure water at room temperature [13]. This involves a highly exothermic self-induced spontaneous surface reaction of the Al-metal with the cold water and ultimately yields a nanocrystalline powder (porous) of the

* Corresponding Author

hydrolyzed Al-metal in $\text{AlO}(\text{OH}) \cdot \alpha \text{H}_2\text{O}$. The value of $\alpha = 0.76$ is determined by thermogravimetric analysis of its dissociation into Al_2O_3 over 300 to 700 K [13].

The phase analysis was carried by studies of X-ray powder diffractograms for the as received and heated samples at selected temperatures in the 500 to 1500 K range. The diffractograms were recorded with the help a P. W. 1710 X-ray diffractometer using a filtered $\text{CoK}\alpha$ radiation of wave length $\lambda = 0.17902 \text{ nm}$. Their microstructures were studied with a JEOL scanning electron microscope with an *in-situ* analysis of their chemical compositions.

3. Results and discussion

A. Thermal stability and phase transformation :

The as prepared $\text{AlO}(\text{OH}) \cdot \alpha \text{H}_2\text{O}$ powder has a porosity $\Phi = 18\%$ as determined by the difference in its theoretical and experimental densities (cf. Table 1). It consists of $\text{AlO}(\text{OH}) \cdot \alpha \text{H}_2\text{O}$ nanoclusters of a monoclinic crystal system of lattice parameters, $a = 0.866 \text{ nm}$, $b = 0.506 \text{ nm}$, $c = 0.983 \text{ nm}$ and $\beta = 94.56^\circ$. Its X-ray

The final Al_2O_3 has a refined microstructure of $\text{AlO}(\text{OH}) \cdot \alpha \text{H}_2\text{O}$ with a considerably enhanced Φ value. A value

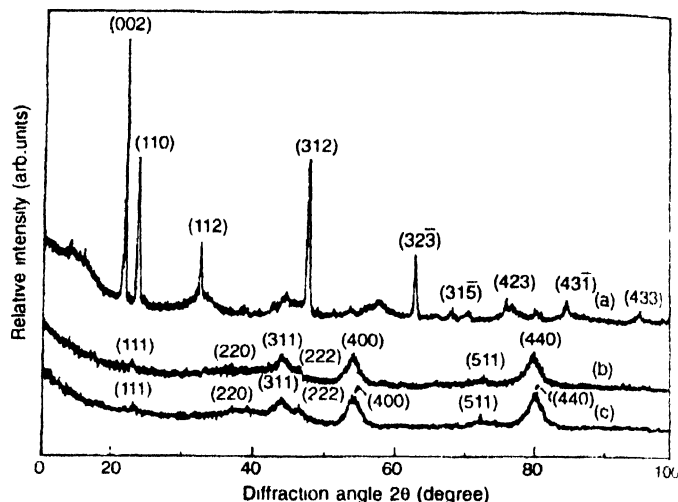


Figure 1. X-ray diffractograms in a controlled thermal decomposition of (a) a porous $\text{AlO}(\text{OH}) \cdot \alpha \text{H}_2\text{O}$ powder in a porous refined Al_2O_3 powder at (b) 750 K for 2 h and (c) 1050 K for 2h in air

Table 1. Al_2O_3 ceramic powders obtained in different polymorphic forms by a controlled thermal dissociation and reconstructive phase transformation of a porous $\text{AlO}(\text{OH}) \cdot \alpha \text{H}_2\text{O}$ powder at elevated temperatures

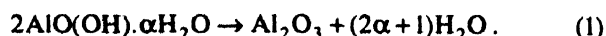
Polymorphic forms	Transformation temperature Porous	Bulk ^a	Crystal structure ^a	Density (g/cm^3) Exp ^b
$\text{AlO}(\text{OH}) \cdot \alpha \text{H}_2\text{O}$	< 310 K		C_{2h}^2 Monoclinic	1.90 (2.25)
$\beta\text{-Al}_2\text{O}_3$	Not observed		$P6_3/mmc$ Hexagonal	(3.24)
$\gamma\text{-Al}_2\text{O}_3$	750 – 1050 K	~ 1070 K	$O_h^7\text{-F}_{23m}$ (fcc, Cubic)	2.20 (3.67)
$\delta\text{-Al}_2\text{O}_3$	Not observed	~ 1270 K	Orthorhombic	(3.20)
$\kappa\text{-Al}_2\text{O}_3$	Not observed	~ 1270 K	$Pna2_1$ Orthorhombic	(3.77)
$\theta\text{-Al}_2\text{O}_3$	1250 – 1350 K	~ 1370 K	$C2/m$ Monoclinic	2.50 (3.62)
$\alpha\text{-Al}_2\text{O}_3$	1400 – 1500 K	~ 1650 K	$D_{3h}^6\text{-R}3c$ Tetragonal	2.98 (3.99)
$\epsilon\text{-Al}_2\text{O}_3$	> 1550 K	> 2200 K	Hexagonal	(4.15)

a) The data are collected from different reports in Refs [1, 3, 5, 13, and 15]

b) The density value calculated from the lattice parameters is included in the parentheses

powder diffractogram, in Figure 1a, exhibits a total of nine well-resolved peaks in significant intensities over 10 to 100° in the $\theta - 2\theta$ scale. The peaks are characteristically sharp with a no significant scattering background throughout the range. However, some weak unresolved broad bands are superposed over the diffractogram of the resolved sharp peaks. Possibly, these are due to a peculiar porous structure of the sample which has very fine pores of size at a nanometer scale. An average crystallite size $D \sim 30 \text{ nm}$ is calculated using the Debye-Scherrer analysis [15] of the peak-widths in the sharp diffraction peaks.

The as-received $\text{AlO}(\text{OH}) \cdot \alpha \text{H}_2\text{O}$ powder is stable as such in ambient atmosphere at room temperatures. On heating over 300 to 1500 K in air, it decomposes into a porous Al_2O_3 powder,



of Φ as large as 40% appears in the sample dehydrated at 800 K. The crystal structures and densities obtained for the samples dehydrated at selected temperatures are given in Table 1. A refined microstructure in the samples is clearly evidenced by broadened peaks in their X-ray diffractograms.

For example, the X-ray diffractograms obtained for the samples dehydrated at early temperatures as 750 K and 1050 K are compared in Figure 1b and 1c. The both samples have the same peaks with similar peak-widths according to an average crystallite size in the 2 to 5 nm range. All these peaks belong to a single nanocrystalline $\gamma\text{-Al}_2\text{O}_3$ phase. This metastable phase is quite stable in its original cubic crystal structure to a temperature as high as 1100 K. The value of the lattice parameters $a = 0.7860 \text{ nm}$ calculated from the positions of these peaks is in a agreement with the bulk $a = 0.7920$ value [16a].

According to the final temperature and other experimental conditions, the Al_2O_3 so obtained assumes a variety of metastable forms. The different phases are stable over different temperatures. Successive reconstructive phase transformations of a low temperature phase to a high temperature phase occur in the $\beta\text{-Al}_2\text{O}_3$, $\gamma\text{-Al}_2\text{O}_3$, $\delta\text{-Al}_2\text{O}_3$, $\kappa\text{-Al}_2\text{O}_3$, $\theta\text{-Al}_2\text{O}_3$, $\alpha\text{-Al}_2\text{O}_3$ and $\epsilon\text{-Al}_2\text{O}_3$ order. In a porous precursor used in this example, these transformation occurs at moderate temperatures if compared to those in a bulk precursor derived from a sol-gel chemistry or other wet methods [14]. For example, the $\alpha\text{-Al}_2\text{O}_3$ phase appears with $\Phi = 25\%$ at as early temperature as 1450 K against 1650 K in the bulk $\text{AlO}(\text{OH}) \cdot \alpha\text{H}_2\text{O}$ (or $\gamma\text{-Al}_2\text{O}_3$) precursor. The pores govern a controlled microstructure of the final phase in a quantum confined size at a nanometer scale. This is not possible with a sol-gel and other wet methods in which the $\text{AlO}(\text{OH}) \cdot \alpha\text{H}_2\text{O}$ precursor molecules are strongly correlated one another through a strong hydrogen bonding. Under identical conditions, these do not disperse in a refined microstructure with a significant Φ value.

The formation and thermal stabilities of the different Al_2O_3 polymorphs are determined by studies of the X-ray diffractograms of those obtained at different temperatures. For example, the diffractograms obtained for the $\theta\text{-Al}_2\text{O}_3$ and $\alpha\text{-Al}_2\text{O}_3$ polymorphs at 1250 K and 1450 K are shown in Figures 2 and 3. A complete list of the different phases observed in this investigation is summarized in Table 1. The most stable phase in this series at a temperature as high as 1500 K is the $\alpha\text{-Al}_2\text{O}_3$ phase. It has a $D_{3d}^6\text{-R}3c$ tetragonal crystal structure of lattice parameters of $a = 0.4102$ nm and $c = 1.3020$ nm. These lattice parameter values are modified a little in comparison with the standard values [16b], $a = 0.4758$ nm and $c = 1.2991$ nm, so that they involve $\sim 25\%$ lower lattice volume. It appears that the pores support the formation of a more distortion free lattice according to its lower volume (or the Gibb's free energy).

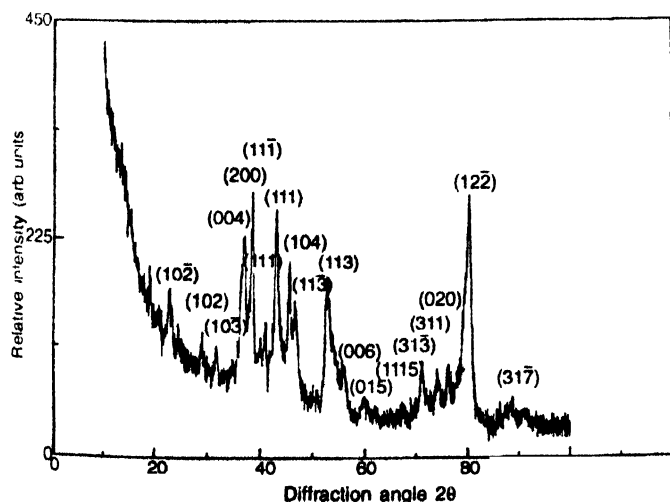


Figure 2. X-ray diffractogram for a porous refined $\theta\text{-Al}_2\text{O}_3$ powder obtained by a controlled thermal decomposition of the porous $\text{AlO}(\text{OH}) \cdot \alpha\text{H}_2\text{O}$ powder at 1250 K for 2 h in air.

B. Microstructure :

We analyzed microstructures of the representative samples with their scanning electron micrographs (SEM). Several micrographs were recorded at different magnifications in an attempt to resolve the size and morphology of the particles and/or crystallites. A

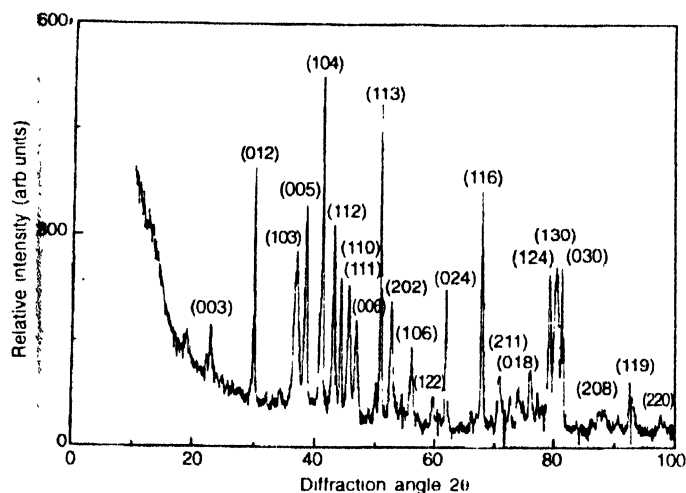


Figure 3. X-ray diffractogram for a porous refined $\alpha\text{-Al}_2\text{O}_3$ powder obtained by a controlled thermal decomposition of the porous $\text{AlO}(\text{OH}) \cdot \alpha\text{H}_2\text{O}$ powder at 1450 K for 2 h in air.

typical set of the SEM micrographs for the sample of $\gamma\text{-Al}_2\text{O}_3$, processed at 750 K for 2h, is shown in Figure 4. The micrographs *a*, *b* and *c* in this figure are recorded at three different magnifications. None of them presents a resolved structure of the particles and/crystallites with a defined size or morphology of them. Perhaps, this is due to a peculiar porous structure of the sample in which the pores and the particles/crystallites are intimately correlated one another at a nanometer scale with a strong macroscopic interaction. As mentioned above, an average crystallite size of 2 to 5 nm is obtained by the peak-widths in the characteristic X-ray diffraction peaks. It seems to be very much consistent with a similar small value in these micrograms. Therefore, it is not resolved in these particular micrograms.

According to the microstructure, the structure as well as the average size of the particles does not change much on raising the processing temperature. For example, a set of three other micrographs for a sample ($\alpha\text{-Al}_2\text{O}_3$) processed at a temperature as high as 1450 K is shown in Figure 5. The structure is a more or less the same as shown above (in Figure 4) for the sample processed at 750 K. An important implications of these results is that the fine pores in the precursor play a vital role in deterring the process of the phase transformation and evolution of the final microstructure. A similar Al_2O_3 sample derived from a sol-gel or other wet methods under identical conditions presents a much coarser microstructure at a micrometer scale [14,17].

4. Conclusions

The work in this article, demonstrates phase transformation in porous aluminas. It is observed that a controlled thermal

decomposition of a nanostructured porous $\text{AlO}(\text{OH}) \cdot \alpha\text{H}_2\text{O}$ precursor in air designs in a porous Al_2O_3 ceramic powder of a refined microstructure. Successive reconstructive phase transformations in the various well-known Al_2O_3 polymorphs (except the $\epsilon\text{-Al}_2\text{O}_3$ one that occurs above 1500 K) appear at

different temperatures in the 500–1500 K range. Unusually, the apparent microstructure of the specimen of refined pores and particles /crystallites does not change much with a variation of the processing temperature in the different polymorphs. The result is very useful in designing of a porous Al_2O_3 and its

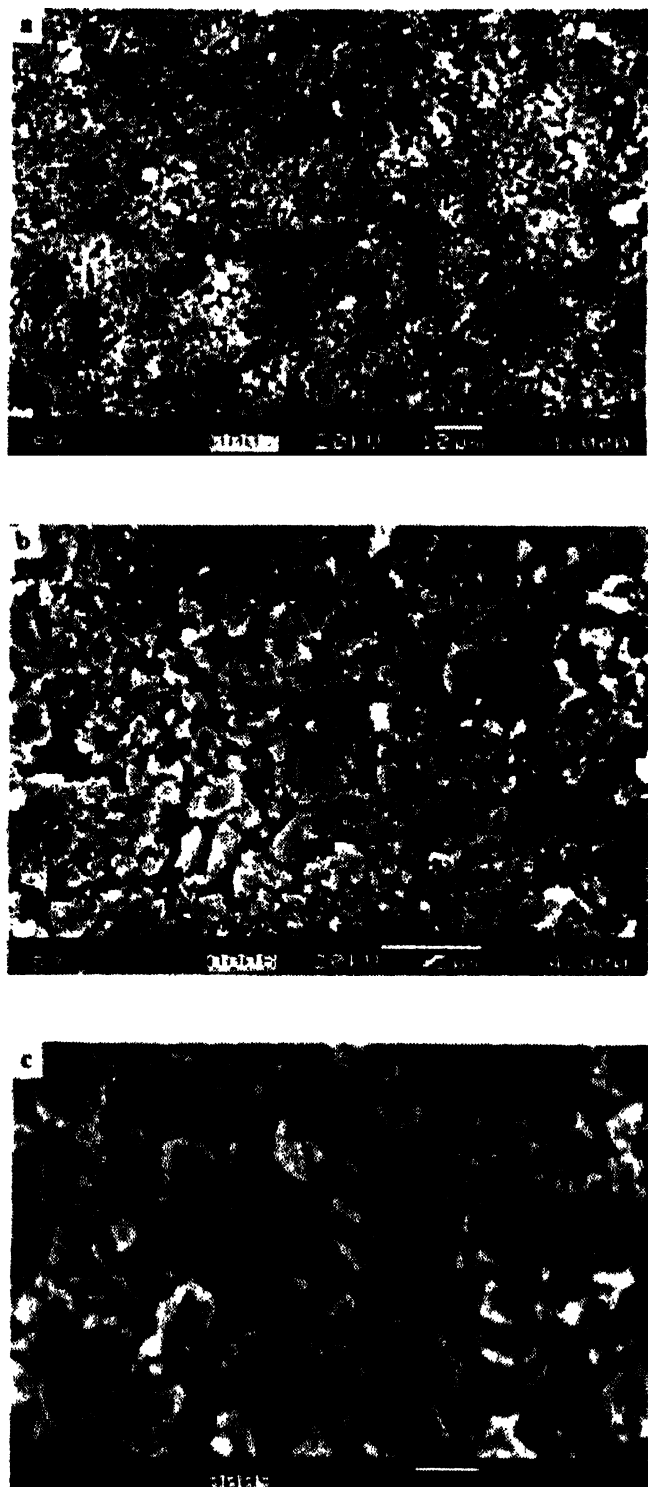


Figure 4. SEM micrographs of a porous refined $\gamma\text{-Al}_2\text{O}_3$ powder obtained by a controlled thermal decomposition of the porous $\text{AlO}(\text{OH}) \cdot \alpha\text{H}_2\text{O}$ powder at 750 K for 2 h in air. The three (a), (b), and (c) micrographs are obtained at three different magnification as marked over them.

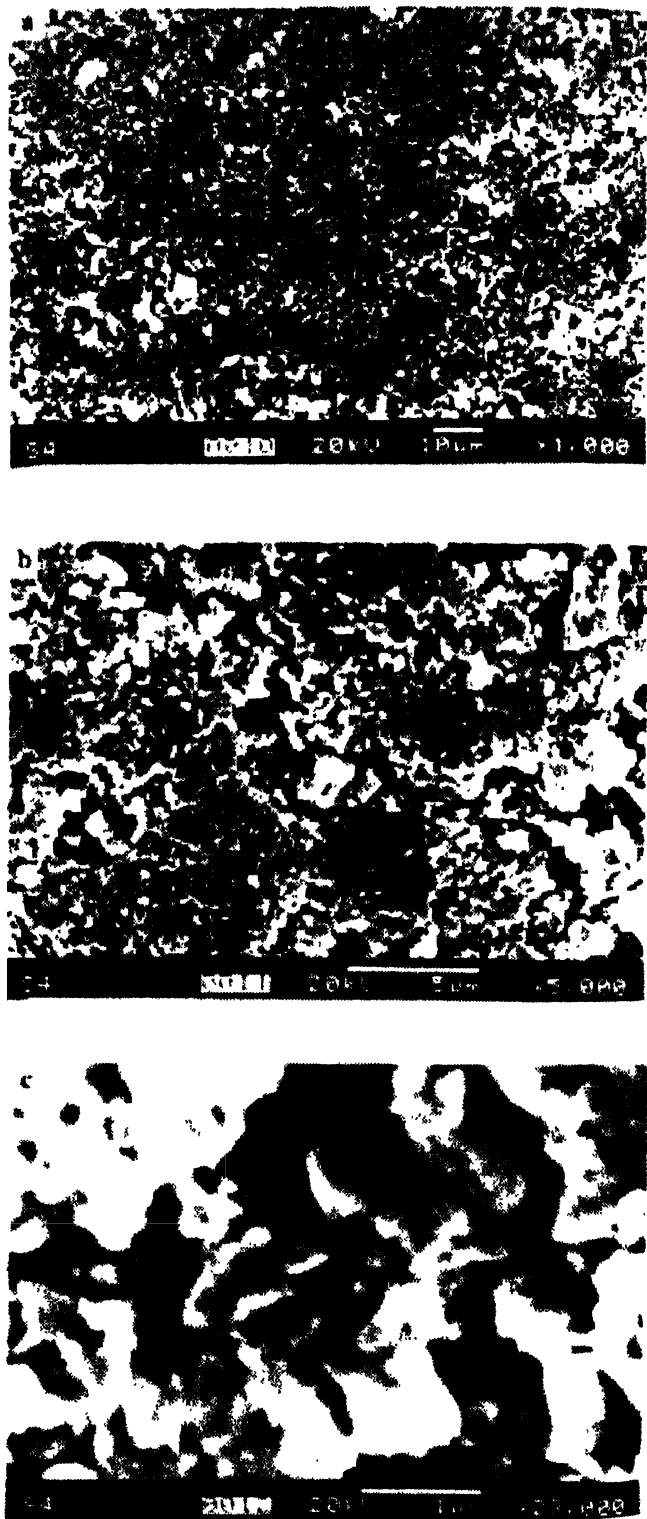


Figure 5. SEM micrographs of a porous refined $\alpha\text{-Al}_2\text{O}_3$ powder obtained by a controlled thermal decomposition of the porous $\text{AlO}(\text{OH}) \cdot \alpha\text{H}_2\text{O}$ powder at 1450 K for 2 h in air. The three (a), (b), and (c) micrographs are obtained at three different magnification as marked over them

composites in a controlled quantum confined particle size at a nanometer scale.

Acknowledgments

This work has been financially supported by a research grant from the Aeronautical Research and Development Board, Government of India.

References

- [1] *Encyclopedia of Glass, Ceramics and Cement* (ed) M Grayson (New York : John Wiley) p24 (1985)
- [2] H G Sowman *Am Ceram. Bull* **67** 1912 (1988)
- [3] Yourdshahyan, U Engberg, L Bengtsson, H I Lundqvist and B Harmer *Phys. Rev.* **B55** 8721 (1996)
- [4] S Ansell, S Krishnan, J K R Weber, J J Felten, P C Nordine, M A Beno, D I Price and M L Saboungi *Phys Rev Lett* **78** 464 (1997)
- [5] S D Mo and W Y Ching *Phys Rev.* **B57** 15219 (1998)
- [6] I Tanaka and H Adachi *Phys. Rev.* **B54** 4604 (1996)
- [7] J C Boettger *Phys. Rev.* **B55** 750 (1997)
- [8] H Yang, N Coombs, I Solokov and G A Ozin *Nature* (London) **381** 589 (1996)
- [9] T Sun and J Y Ying *Nature* (London) **389** 704 (1997)
- [10] W Cai, Y Zhang, J Jai and L. Zhang *Appl. Phys. Lett.* **73** 2709 (1998)
- [11] S Kondoh, Y Iwamoto, K Kikuta and S Hirano *J. Amer. Ceram. Soc.* **82** 209 (1999)
- [12] S Ram, T B Singh and L C Pathak *Phys. Stat. Sol. (a)* **165** 151 (1998)
- [13] S Ram and S Rana *Mat. Lett.* (in press)
- [14] B E Yoldas *J. Appl. Biotech.* **3** 803 (1972)
- [15] L Azaroff *Elements of X ray Crystallograph* (New York McGraw Hill) p 557 (1968)
- [16] *X-ray Powder JCPDS Diffraction Files* (a) 10-425, and (b) 10-173, (c) 4-0877, (d) 4-0878, (e) 10-414, (f) 23-1009, and (g) 21-10
- [17] M Chatterjee, D Enkhuvshin, B Siladitya and D Ganguli *J. Mater. Sci.* **33** 4937 (1998)